Supplementary Information

One-Step additive manufacturing of Ni-Mn-Sn alloys with large elastocaloric effect

Wen Sun,[ab] Hanyang qian,[ab] Qi Fu,[c] Mingxiao Zhang,[ab] Juan Cheng,[d] Zhaojun Mo,[c] Jian Liu,[e] W. Li,[f] and Guowei Li,*[ab]

[a] Zhejiang Province Key Laboratory of Magnetic Materials and Application Technology, Ningbo Institute of Materials Technology and Engineering, Chinese Academy of Sciences, Ningbo 315201, China.

[b] University of Chinese Academy of Sciences, Beijing 100049, China.

[c] Key Laboratory of Rare Earths, Ganjiang Innovation Academy, Chinese Academy of Sciences, Ganzhou 341119, China.

[d] Baotou Research Institute of Rare Earths, Baotou, 0472, China.

[e] School of Materials Science and Engineering, Shanghai University, Shanghai 200444, China.

[f] CISRI & NIMTE Joint Innovation Center for Rare Earth Permanent Magnets.

* Authors to whom correspondence should be addressed: Guowei Li, E-mail addresses: liguowei@nimte.ac.cn

Table S1 L-PBF parameters for the P50 - P180 samples and relative density measured by micro-CT.

Samples	Scanning strategy	Laser power P (W)	Scanning speed v (mm s^{-1})	Hatching spacing H (μm)	Layer thickness d (μm)	Energy density E (J mm^{-3})	Relative density ρ (%)
P_{50}	unidirectional strategy	50	1000	100	20	25	92.45
P_{60}		60	1000	100	20	30	95.26
P_{100}		100	2000	100	20	25	96.68
P_{120}		120	2000	100	20	30	95.44
P_{150}		150	3000	100	20	25	98.20
P_{180}		180	3000	100	20	30	93.58

Table S2 The elemental compositions of the samples via the ICP-OES test.

Element	Ni (at. %)	Mn (at. %)	Sn (at. %)
Powder	43.88	43.79	12.33
P50	44.53	42.81	12.66
P150	44.85	42.52	12.62
P180	45.62	41.78	12.60

Table S3 The statistics of cracks. The n1 and n2 are the numbers of red cracks and purple/blue cracks, respectively. The V1, V2 and V are the volumes of red crack, purple/blue crack and sample, respectively.

Samples	Red cracks			Purple and blue cracks		Total crack defects
	n1	n1/(n1+n2) （%）	V1/V （%）	n2/(n1+n2) （%）	V2/V （%）	(V1+V2)/V (%)
P_{50}	7	0.012	3.34	99.988	3.11	6.45
P_{60}	1	0.020	3.34	99.980	1.17	4.51
P_{100}	1	0.002	2.16	99.998	1.01	3.17
P_{120}	1	0.014	3.61	99.986	0.83	4.44
P_{150}	1	0.005	0.36	99.995	1.21	1.57
P_{180}	1	0.005	2.67	99.995	1.11	3.78

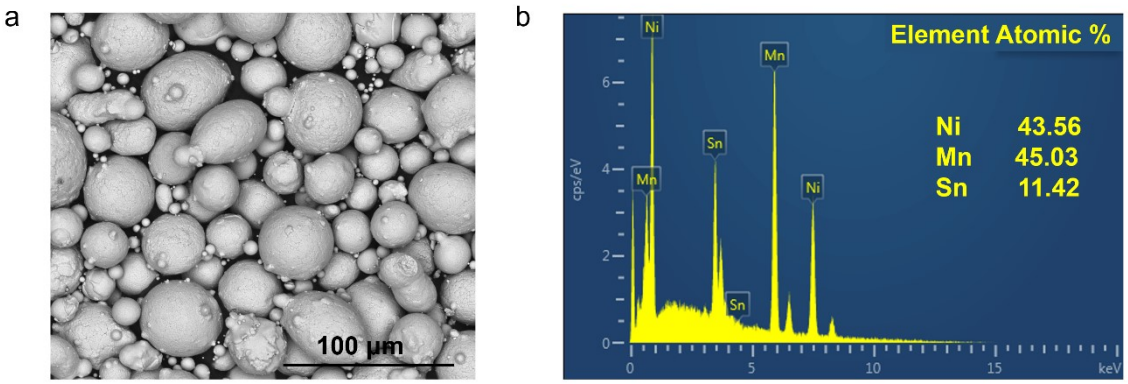

Fig. S1 (a) Backscattered scanning electron morphology (SEM) and (b) energy dispersive spectrum (EDS) of Ni-Mn-Sn powder for 3D printing.

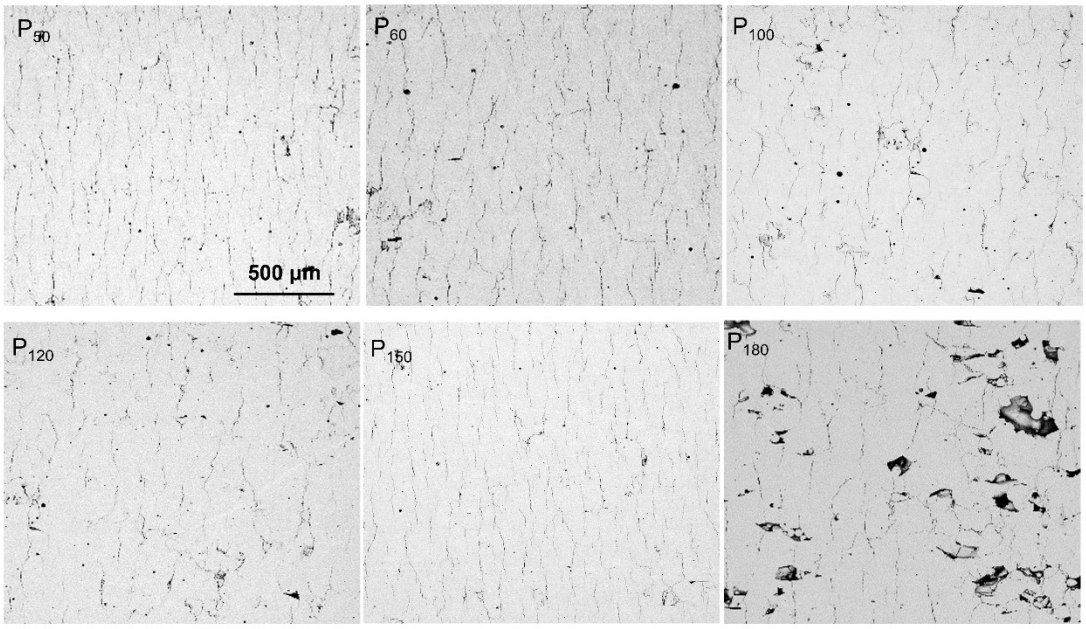

Fig. S2 Backscattered SEM microstructures in the TD - BD plane (perpendicular to the SD) in P_{50} - P_{180} samples.

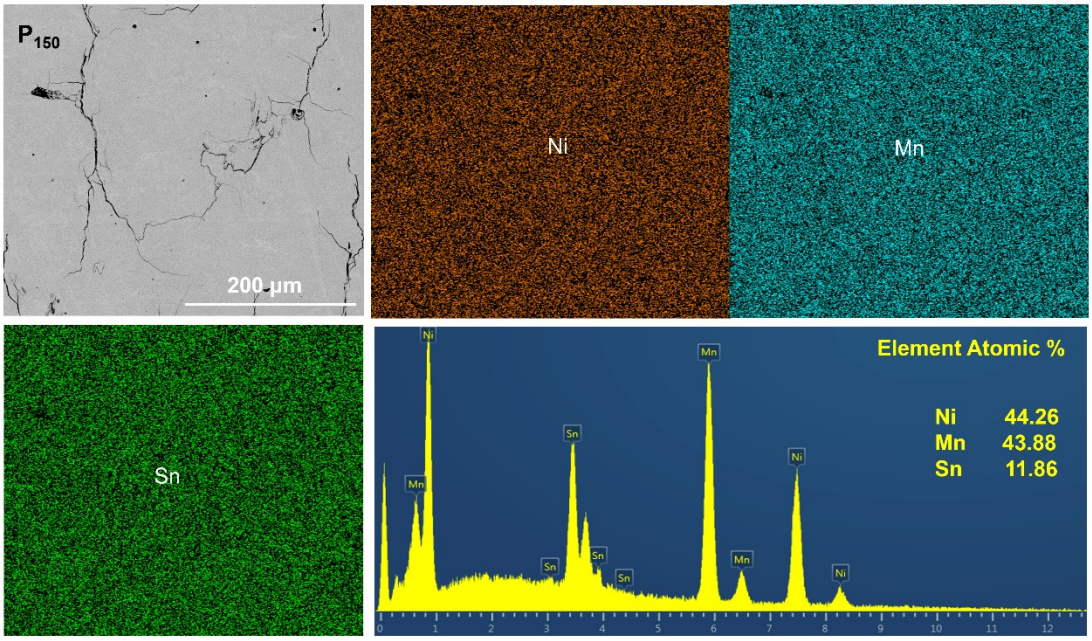

Fig. S3 The SEM and Ni, Mn, Sn elemental mapping images and EDS of P_{150} sample.

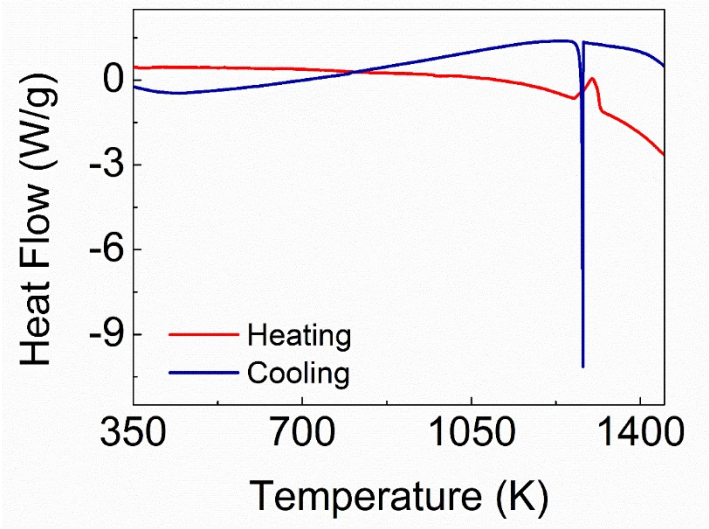

Fig. S4 Differential thermal analysis (DTA) curves of the P_{150} samples.

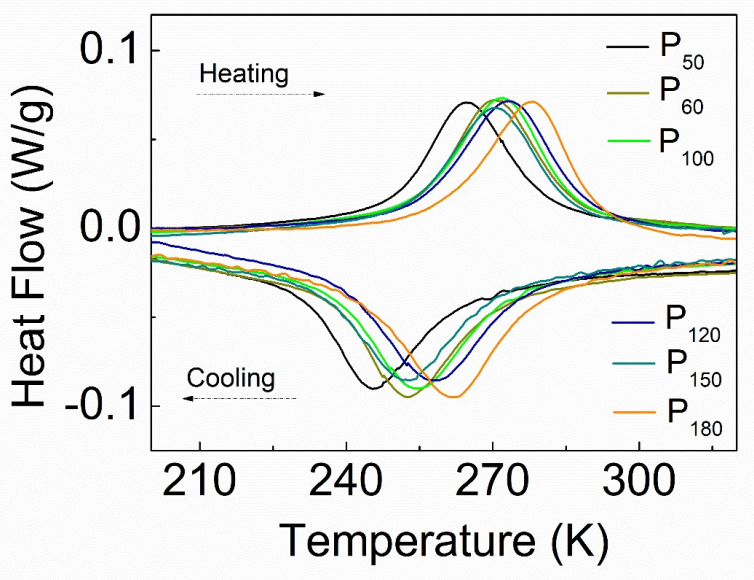

Fig. S5 DSC curves of alloys with different laser power.

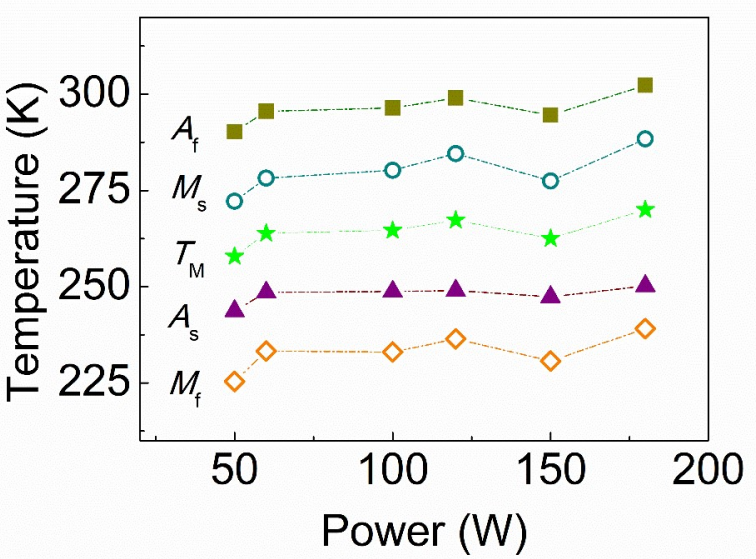

Fig. S6 Transformation characteristic temperature (M_s, M_f, A_s, A_f) and average characteristic temperatures ($T_M = (M_s + M_f + A_s + A_f) / 4$) in L-PBF Ni-Mn-Sn alloys.

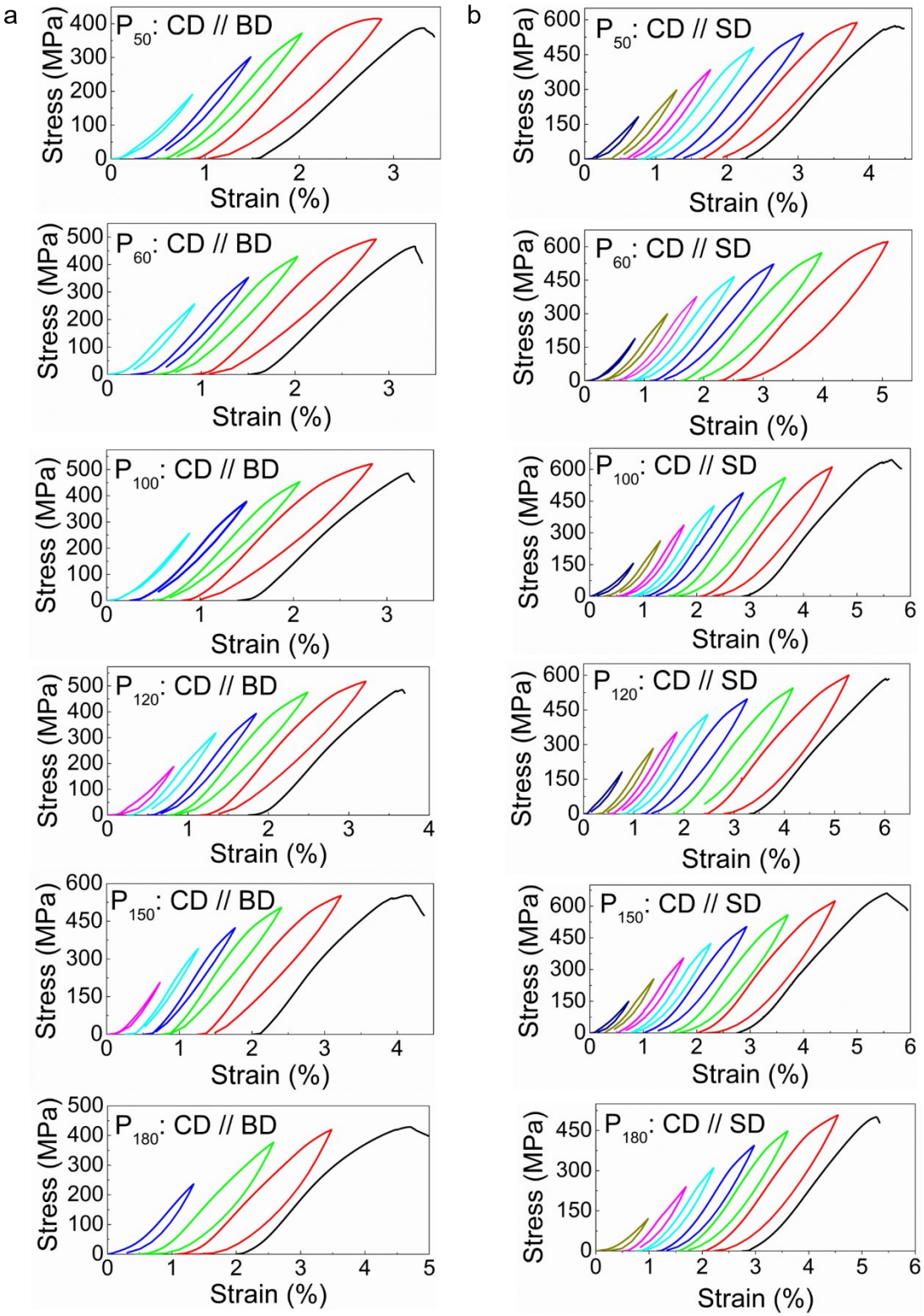

Fig. S7 Stress - strain curves at room temperature under compression along the (a) BD and (d) SD in P_{50} - P_{180} samples.

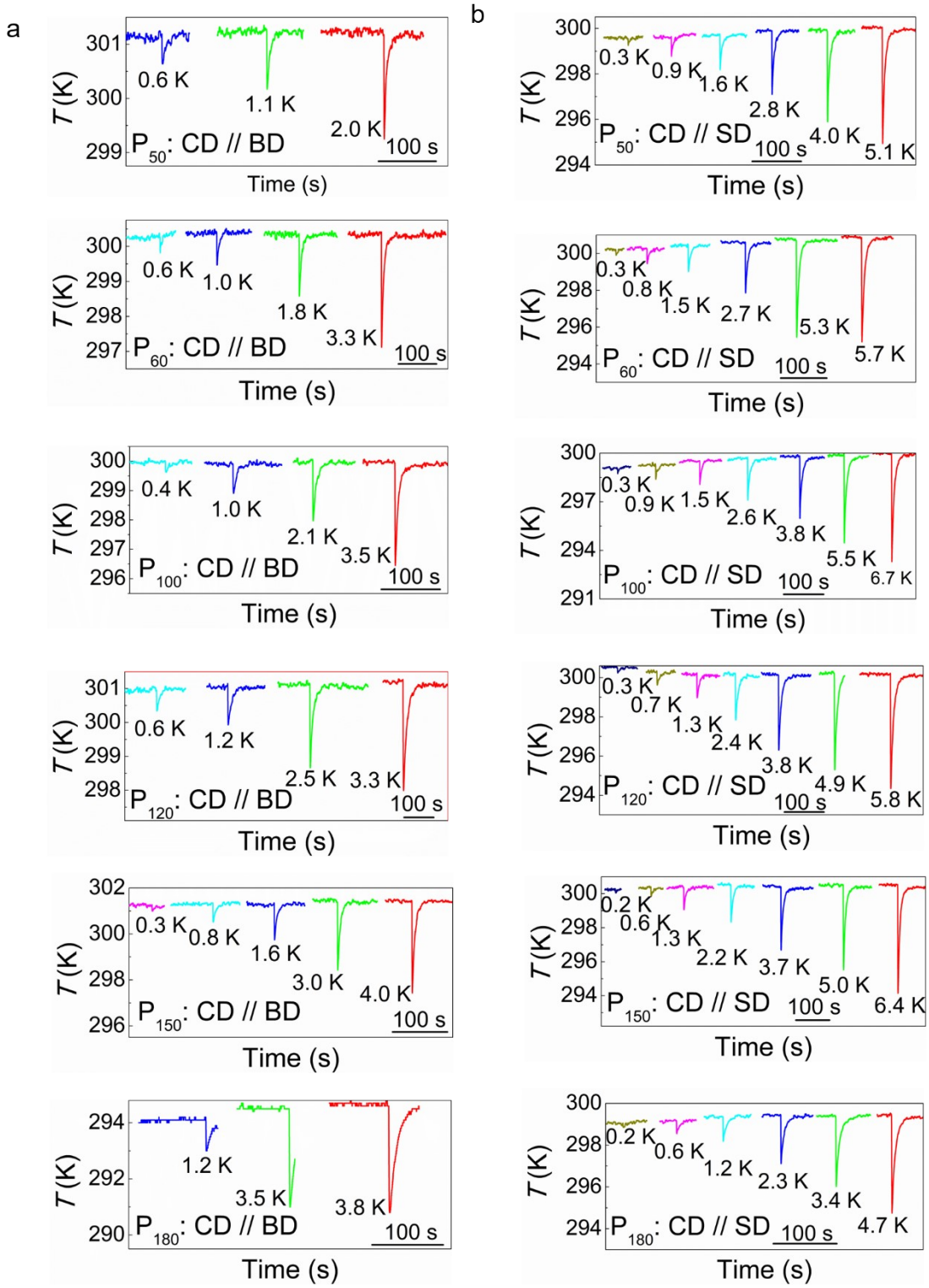

Fig. S8 corresponding elastocaloric temperature changes upon unloading in Fig. S7. (a) unloading temperature changes after compression along the BD and (b) after compression along SD in P_{50} - P_{180} samples.

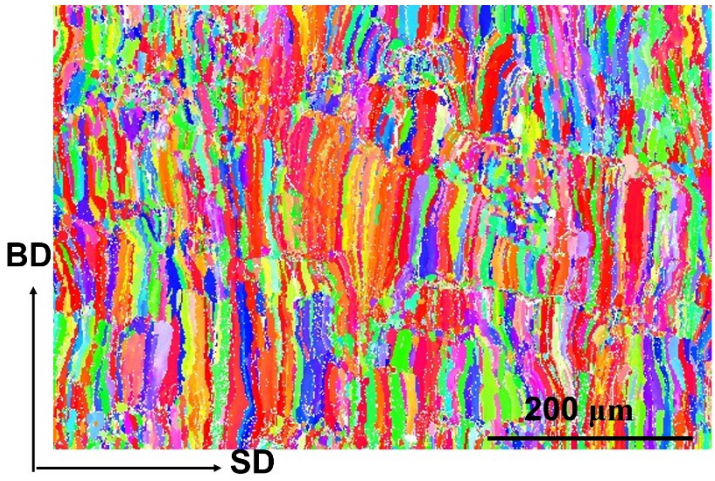

Fig. S9 EBSD mapping of sample P_{180} in the building - scanning direction (BD - SD) plane. the Inverse Pole Figures are plotted with the <001> directions parallel to the SD.

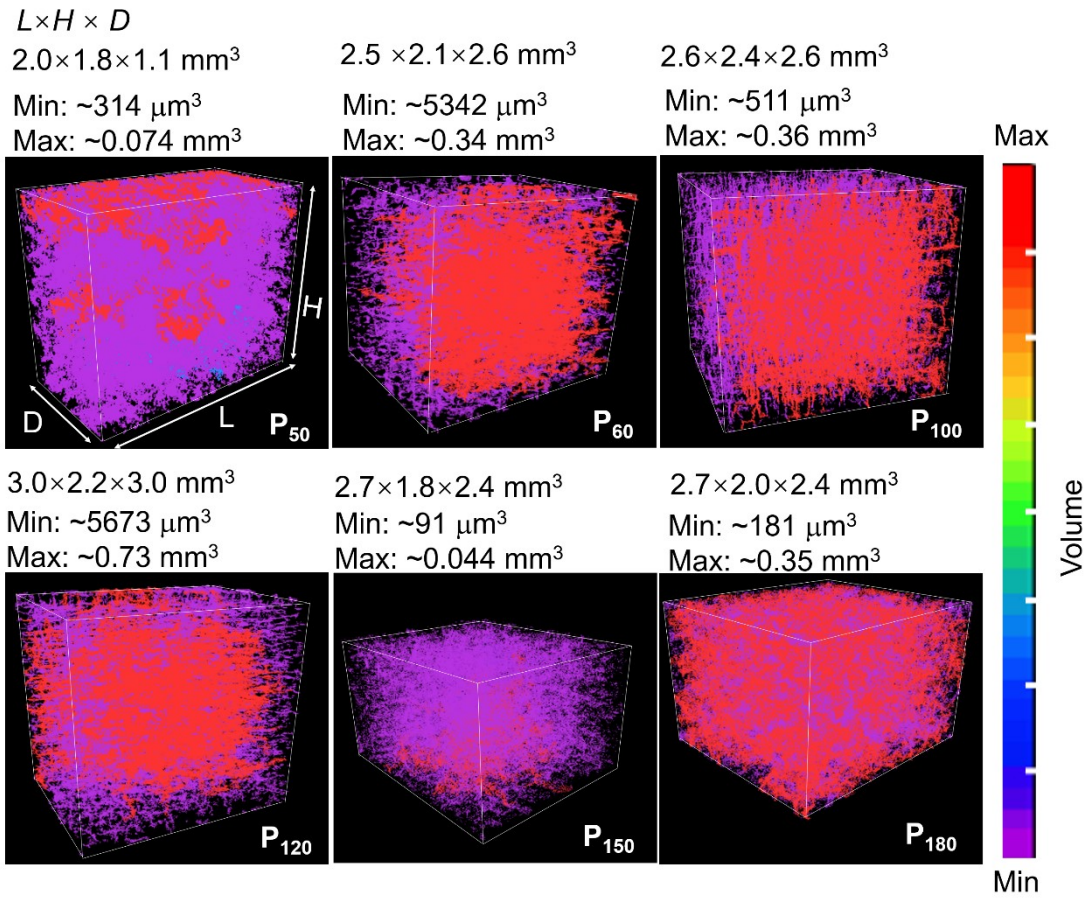

Fig. S10 3D reconstructed morphology of cracks via Mico-CT in L-PBF samples. The different colors represent the difference in the volume of cracks and pores.

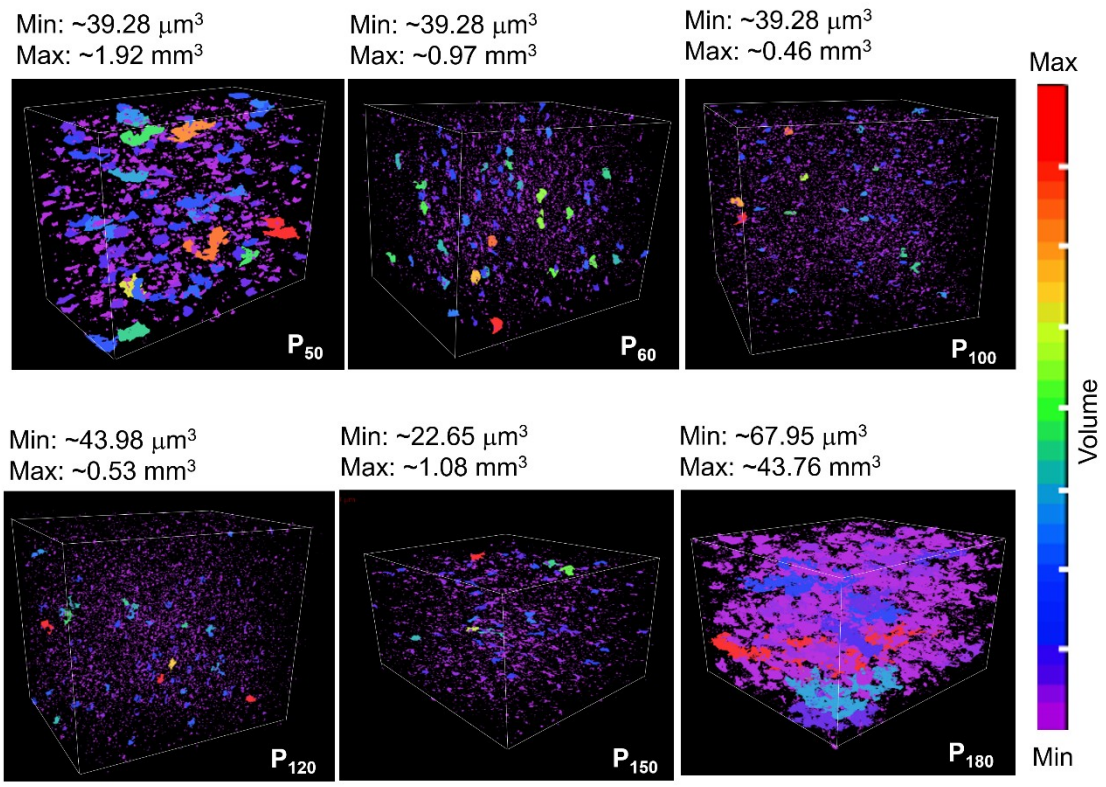

Fig. S11 3D reconstructed morphology of pores via Mico-CT in L-PBF samples. The different colors represent the difference in the volume of cracks and pores.

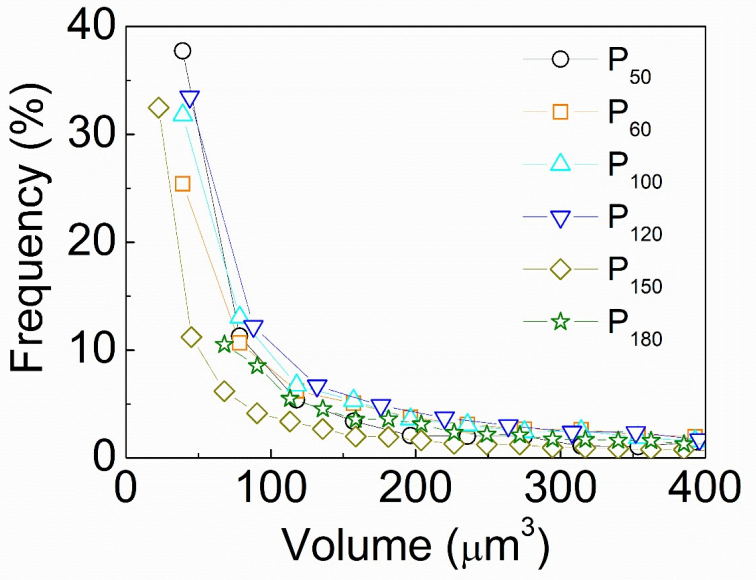

Fig. S12 Occurrence frequency of pore defects with different volumes in the L-PBF Ni-Mn-Sn samples.

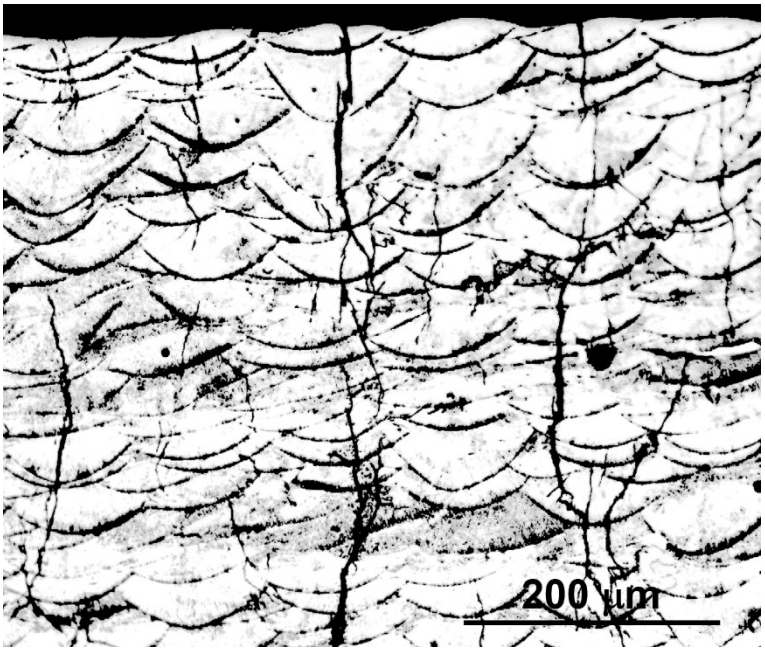

Fig. S13 The optical microscope image of melt pools in P_{150} sample.

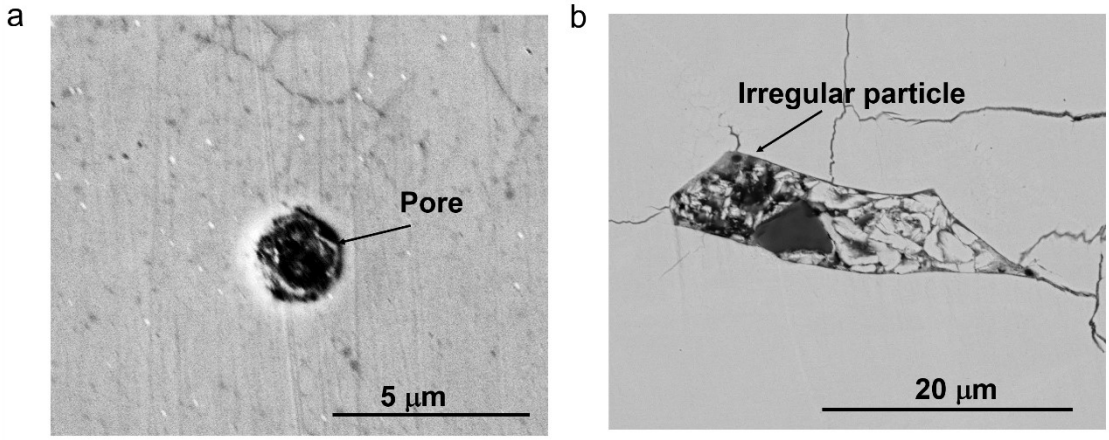

Fig. S14 (a) SEM image of gas pores defects. (b) SEM image of pore formed by spray particles without melting.

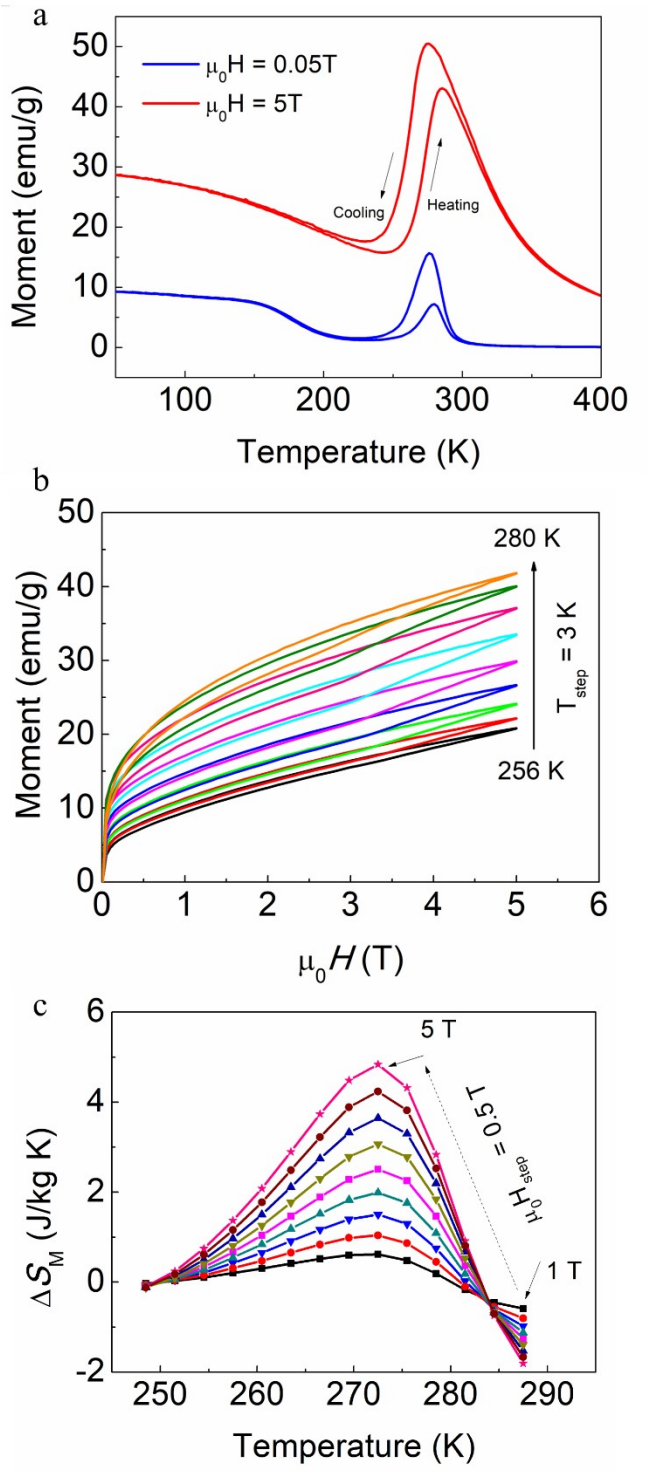

Fig. S15 (a) Magnetization vs. temperature (*M-T*) and (b) magnetization vs. field (*M-H*) curves for P_{180} sample. The entropy changes ΔS_M were calculated from magnetization isothermals in (b) and plot as a function of temperature under different magnetic field changes.